



Bulletin of the Mineral Research and Exploration

<http://bulletin.mta.gov.tr>



GEOCHEMICAL CHARACTERISTICS AND RARE-EARTH ELEMENT DISTRIBUTIONS OF KOZBUDAKLAR W-SKARN DEPOSIT (BURSA, WESTERN ANATOLIA)

Ayşe ORHAN^{a*} and Halim MUTLU^b

^a*Nevşehir Hacı Bektaş Veli University, Department of Geological Engineering, Nevşehir. orcid.org/0000-0001-8103-5376*

^b*Ankara University, Department of Geological Engineering, Gölbaşı, Ankara. orcid.org/0000-0002-4100-1363*

Research Article

Keywords:

Scheelite Mineralization,
Rare-Earth Elements,
Kozbudaklar, Bursa,
Western Anatolia.

ABSTRACT

The Kozbudaklar W-skarn deposit occurs along the contact between Eocene Topuk granitoid and Triassic İnönü marble in Tavşanlı Zone. In the study area, the endoskarn is represented by plagioclase-pyroxene and exoskarn zone which is characterized by pyroxene, pyroxene-garnet, garnet and garnet-pyroxene skarn facies. According to major oxide element contents, exoskarn is of calcic character. In pyroxene and pyroxene-garnet skarn facies, tungsten and molybdenum abundances vary between 434-5507 ppm (mean 2330 ppm) and 8 - 90 ppm (mean 40 ppm). In the garnet and garnet-pyroxene skarns, concentrations of these elements are 271 - 7616 ppm (mean 2486 ppm) and 7 - 493 ppm (mean 107 ppm), respectively, and molybdenum concentration is increased. ΣREE contents of the Topuk granitoid, endoskarn, exoskarn and İnönü marble are in the range of 75.8 to 158.9 ppm (mean 106.2 ppm), 75.8 to 171.5 ppm (mean 114.6 ppm), 3.5 to 290.8 ppm (mean 48.7 ppm) and 2.3 to 15.3 ppm (mean 6.1 ppm), respectively. Although ΣREE concentrations of skarn zones are higher than those of Topuk granitoid and İnönü marble, ΣREE concentrations of tungsten-rich samples are significantly depleted. In areas of scheelite mineralization, REE trends and Eu anomalies display two different patterns. REE trends, HREE enrichments and negative Eu anomalies of pyroxene and pyroxene-garnet skarn facies exhibit similarities with Topuk granitoid. In these skarn facies, tungsten-rich samples are represented by a Ce depletion and low Eu/Eu* (Eu/Eu* = 0.56-0.88). Garnet and garnet-pyroxene skarn facies are characteristic with a convex LRRE pattern, maximum Pr and Nd concentrations and positive Eu anomalies. Ce-enrichment and high Eu/Eu* ratios (Eu/Eu* = 1.45 - 4.18) are observed in tungsten-rich samples. Considering the molybdenum enrichments and REE pattern, scheelite mineralization in the Kozbudaklar W-skarn deposit can be said to have developed at two different high temperature phases. In the first-phase mineralization was formed by early magmatic fluids under moderate oxidant conditions whilst the second-phase scheelite mineralization was formed under increasing oxidant conditions.

Received Date: 24.11.2016

Accepted Date: 08.02.2017

1. Introduction

Rare earth elements (REE) which are widely used for petrological classification of magmatic rocks have been recently commonly applied to assessment of several parameters including the degree of fluid-rock interaction, the source of fluids, pH variations, various agents in fluids (e.g. Cl, SO₄, CO₃), reducing mechanisms and temperature (Michard, 1989; Bau, 1991; Vander Auwera and Andre, 1991; Lottermoser, 1992; Whitney and Olmsted, 1998; Bi et al., 2004; Oyman et al., 2013; Song et al., 2014). Results of such studies showed that changes in oxidation conditions, pH and temperature exert a primary control on REE

distributions and particularly Eu and Ce concentrations. Fluid-rock interaction at low temperature may disturb REE pattern of whole rock whilst interaction at high-temperature has rather a limited effect on REE distribution. It was shown that pH decrease in fluids (acidic conditions) increases REE concentrations (Lottermoser, 1992) and fluid-rock interaction under high temperature and changes in oxidation conditions raise the Eu/Eu* ratio (Bau, 1991; Whitney and Olmsted, 1998; Bi et al., 2004; Oyman et al., 2013; Song et al., 2014). It is also reported that depletion of REEs in the source rock or fluid-rock interaction triggered by fractionation of magmatic rocks have a limited effect on REE patterns (Bau, 1991).

* Corresponding author: Ayşe ORHAN, ayse.orhan@nevsehir.edu.tr
<http://dx.doi.org/10.19111/bulletinofmre.305992>

Studies on W-skarn systems indicated that magma chemistry, host rock composition, skarn formation depth, reducing conditions and change in temperature are important parameters (Sato, 1980; Kwak and Tan, 1981; Newberry, 1982; Brown et al., 1985; Gerstner et al., 1989; Fonteilles et al., 1989; Zaw and Singoyi, 2000; Timon Sanchez et al., 2009; Orhan, 2017). It was stated that W-skarn deposits, which are classified as “reducing” and “oxidizing” types with respect to pressure and oxidation conditions, generally favour high-temperature systems (Einaudi et al., 1981; Meinert et al., 2005). According to these authors, reducing W-skarn systems of economic importance are represented by ferrous (e.g. hedenbergite, grossular) minerals at early (prograde) stage whilst oxidizing type skarn systems are enriched in ferric minerals (e.g. diopside, andradite). It was asserted that scheelite grade in both skarn systems attains an economic size with increasing degree of fluid-rock interaction and hydrous mineral abundance at the late (retrograde) stage (Brown et al., 1985; Zaw and Singoyi, 2000).

In this study, based on major oxide, trace and rare earth element characteristics of Kozbudaklar W-skarn deposit (Keles, Bursa) (Figure 1), the source of metasomatic mineralizing fluids, fluid-rock interaction, oxidation conditions and temperature variations were investigated. Previous studies were carried out to examine general geological features (Lisenbee, 1972; Okay, 1985; 2011; Orhan et al., 2015) and the ore potential of the region (Romberg, 1938; MTA, 1965; Pehlivan, 1987) and investigate the petrogenetic properties of Topuk granitoid (Harris et al., 1994; Delaloye and Bingöl, 2000; Okay and Satır, 2006; Altunkaynak, 2007; Orhan et al., 2014a). Romberg (1938) is the first to mention the occurrence of skarn minerals (e.g. pyroxene, garnet, epidote and vesuvianite) and scheelite, pyrrhotite, molybdenite and magnetite mineralizations around the Kozbudaklar village. Reserve and grade of scheelite deposit are estimated 238.000 tons and 0.31% WO_3 (MTA, 1965). In a recent study by Orhan (2017), P-T conditions and composition of ore-forming fluids have been discussed. Orhan (2017) described at least four stages in the evolution of Kozbudaklar scheelite skarn deposit and proposed that scheelite mineralization occurred along the contact of Topuk pluton (in the proximal zone) in the prograde stage (I and II) rather than retrograde stage.

In the present study, based on previously described skarn facies (Orhan, 2017), the character of exoskarn

in the Kozbudaklar scheelite skarn deposit (calcitic or dolomitic) was determined using major oxide and trace element contents from various skarn facies. Comparing REE trends of Topuk granitoid and İnönü marble, the source of metasomatic fluids, the degree of fluid-rock interaction, oxidation conditions and temperature changes were also discussed.

2. Analytical Methods

Major oxide, trace and rare earth element analyses of samples from İnönü marble and skarn facies were carried out ACME (Canada) laboratories. The locations of samples are shown in Figures 1 and 2. Before the analysis, about 100 g from each sample was cleaned. Major oxides and some trace elements (Ba, Ni, Sr, Sc, Y and Zr) were analyzed with ICP-ES whilst rare earth elements were determined by ICP-MS method. During the analyses CANMET SY-4 and STD SO-17 standards were used and accuracy of major oxide and trace element analyses are 0.001–0.04% and 0.01–0.5 ppm, respectively.

3. General Geology

The İzmir-Ankara Suture Zone which defines the closure of Neotethys Ocean divides the northwest Anatolia into two parts – Sakarya Continent at north and Anatolide-Tauride Platform at south (Okay et al., 1998). The Topuk granitoid is located in the Tavşanlı Zone at north of Anatolide-Tauride Block in northwest Anatolia (Figure 1). In the Tavşanlı Zone four tectono-stratigraphic units have been described (Okay, 2011). These units from bottom to the top are the Orhaneli group consisting of terrestrial rocks, ophiolitic mélange and/or ophiolites, Eocene sedimentary rocks and Eocene granitoids. In the study area, Paleozoic-Mesozoic Kocasu formation of Orhaneli group, Triassic İnönü marble, Upper Cretaceous Orhaneli Ophiolite and Eocene Topuk granitoid are exposed (Figure 1).

The Kocasu formation at the base of Orhaneli group is composed of quartz-mica schist, quartz-calc schist and chlorite schist and distributed along southern and northern parts of Tavşanlı Zone (Okay and Kelley, 1994; Okay, 2004; Orhan et al., 2015). The mineral associations of quartz + phengite + jadeite + chloritoid + lawsonite + glaucophane and muscovite + biotite + chlorite + quartz + albite in the Kocasu formation indicate P-T conditions of 20 ± 2 kbar and $430 \pm 30^\circ\text{C}$ implying a blueschist metamorphic facies (Harris et al., 1994; Okay, 2011). $^{40}\text{Ar}/^{39}\text{Ar}$ dating

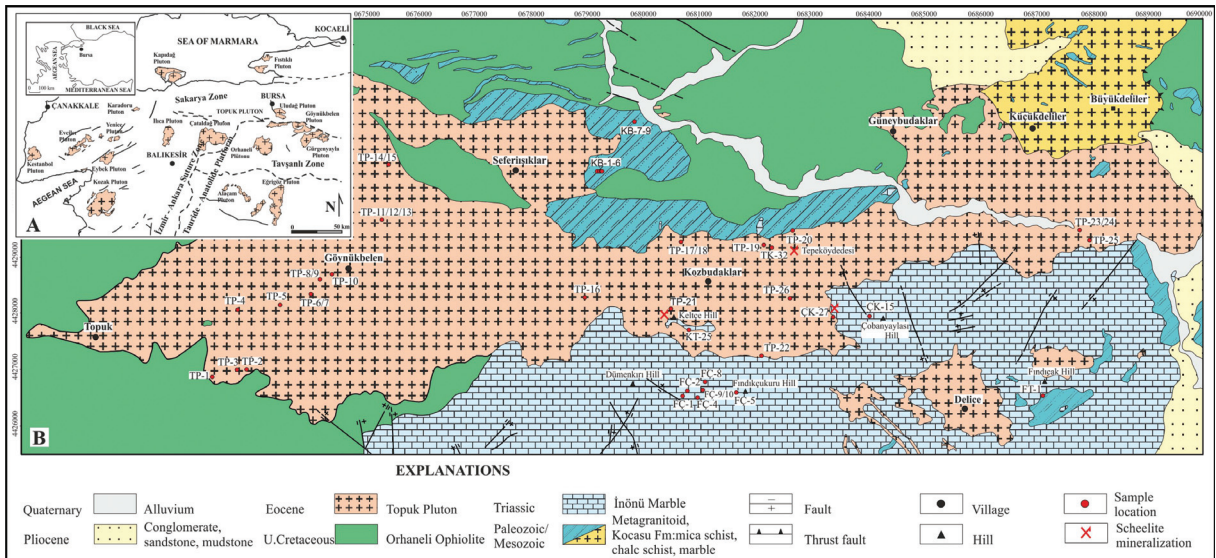


Figure 1- a) Tertiary plutonic rocks of Northwest Anatolia (simplified from MTA, 2002) and b) Geological and sample location map of the study area (MTA, 1973).

from phengite and glaucophane minerals yields that metamorphism was continued in the time interval of 108 to 88 Ma (Harris et al., 1994). The İnönü marble consisting of pure calcite crystals gradually changes to the schists of Kocasu formation. The calcitic marble is white colored, distinctly laminated and grain size is increased towards the skarn zone and pluton contact.

The Orhaneli ophiolite which is a relict mass of the Neotethys Ocean at northwest Anatolia has been thrust onto the Paleozoic-Mesozoic metamorphic rocks (Lisenbee, 1972; Örgün, 1993). The unit is composed chiefly of peridotites and partly of gabbro and pyroxenite dykes (Örgün, 1993; Emre, 1996; Okay, 2011). Paleontological descriptions on radiolarites within ophiolitic mélangé at northern part of Tavşanlı Zone yield Triassic-Cretaceous age for the unit (Tekin et al., 2002).

The Topuk granitoid, which is one of the intrusions formed subsequent to closure of Neotethys Ocean in the late Cretaceous (Şengör and Yılmaz, 1981) and collision between Anatolide-Tauride and Sakarya Continent, comprises an area of about 55 km² (Figure 1). The E-W trending and ellipsoidal-shaped granitoid was intruded the Paleozoic-Mesozoic metamorphics, Triassic marble and Upper Cretaceous ophiolitic rocks. The mineral assemblage of andalusite + cordierite + biotite + muscovite + K-feldspar + plagioclase at the contact of plutonic and metamorphic rocks implies that metamorphism took place at pressure of 2±1 kbar and temperature of 575±50°C (Okay and Satır, 2006).

At the contact between pluton and Triassic marble around the Kozbudaklar village, skarn zone has been developed as irregular roof pendants.

The Topuk granitoid is recognized in gray to light gray color and exhibits moderate-coarse equigranular texture. The host rock of pluton is granodiorite which contains spherical/ellipsoidal mafic mineral enclaves (MME) of monzodiorite/monzogabbro composition. The granitoid is often cut by porphyric granodiorite, granitic aplite and quartz veins at marginal facies and contain xenolith fragments (Orhan et al., 2014a; 2015). Alteration is quite common at the contacts of granitoid with other units. Particularly towards the skarn contacts, grain size of granitoid is reduced, feldspar content is increased and it is repeatedly cut by quartz veins. According to results of geochemical and isotopic analyses, the Topuk granitoid is a product of arc magmatism formed in an active continental margin and mantle and subduction-related melts greatly contributed to the magma development (Harris et al., 1994; Altunkaynak, 2007; Orhan et al., 2014a). K-Ar ages on various mineral separates from the pluton are reported 43.0±2.7 Ma for biotite, 49.8±2.7 Ma for orthoclase (Bingöl et al., 1982) and 47.8±4 Ma for hornblende (Lisenbee, 1972).

4. Mineralogical Characteristics of Kozbudaklar Skarn Deposit

Detailed morphologic and mineralogic observations of skarn zones and micro probe analysis

on calc-silica and ore minerals (e.g. garnet, pyroxene, scheelite and plagioclase) at Kozbudaklar have been reported by Orhan (2017). Scheelite in the skarn zone is recognized at northeast (Tepeköydedesi), southeast (Çobanyaylası) and southwest (Kepçe Hill) parts of the Kozbudaklar village (Figure 2). According to Orhan et al. (2014b) and Orhan and Mutlu (2015), both endo and exoskarn zones have been developed with respect to type of rock replaced.

The endoskarn zone at the pluton contact is widely exposed at northeast of the area. The zone with a width varying from 75 to 165 m is composed chiefly of clinopyroxene (Hd₉₅₋₉₆) and plagioclase (An₅₅₋₆₄) (Table 1). Based on mineral abundances this zone has been described as plagioclase-pyroxene (Plg-Pyx) skarn. The exoskarn zone was developed as monomineralic zones, lenses and irregular bands at the contact of pluton and/or endoskarn (in proximal zone) and within the marble (in distal zone). The contacts of

exoskarn zone with pluton, endoskarn zone and marble are quite sharp. The exoskarn zone has a limited distribution at northeast and its width varies from 2 to 112 m at northeast and from 125 to 150 m at south. Considering mineral abundances, textural properties and mineral compositions, four different skarn facies have been recognized in the exoskarn zone (Table 1). All the skarn zones are composed mainly of garnet and/or clinopyroxene but textural characteristics of these minerals show differences. Pyx (pyroxene) skarn is observed only at Tepeköydedesi location whilst Pyx-Gar (pyroxene-garnet) skarn is exposed at Tepeköydedesi, Çobanyaylası and Kepçe Hill locations. Pyx skarn has been developed at endoskarn contact (in proximal zone). Pyx-Gar skarn is found in Pyx skarn (in proximal zone) at the Tepeköydedesi location and along marble contact (in distal zone) at Çobanyaylası and Kepçe Hill locations. Pyroxene and garnet are accompanied by scheelite in the proximal zone and by wollastonite in the distal zone. Garnets

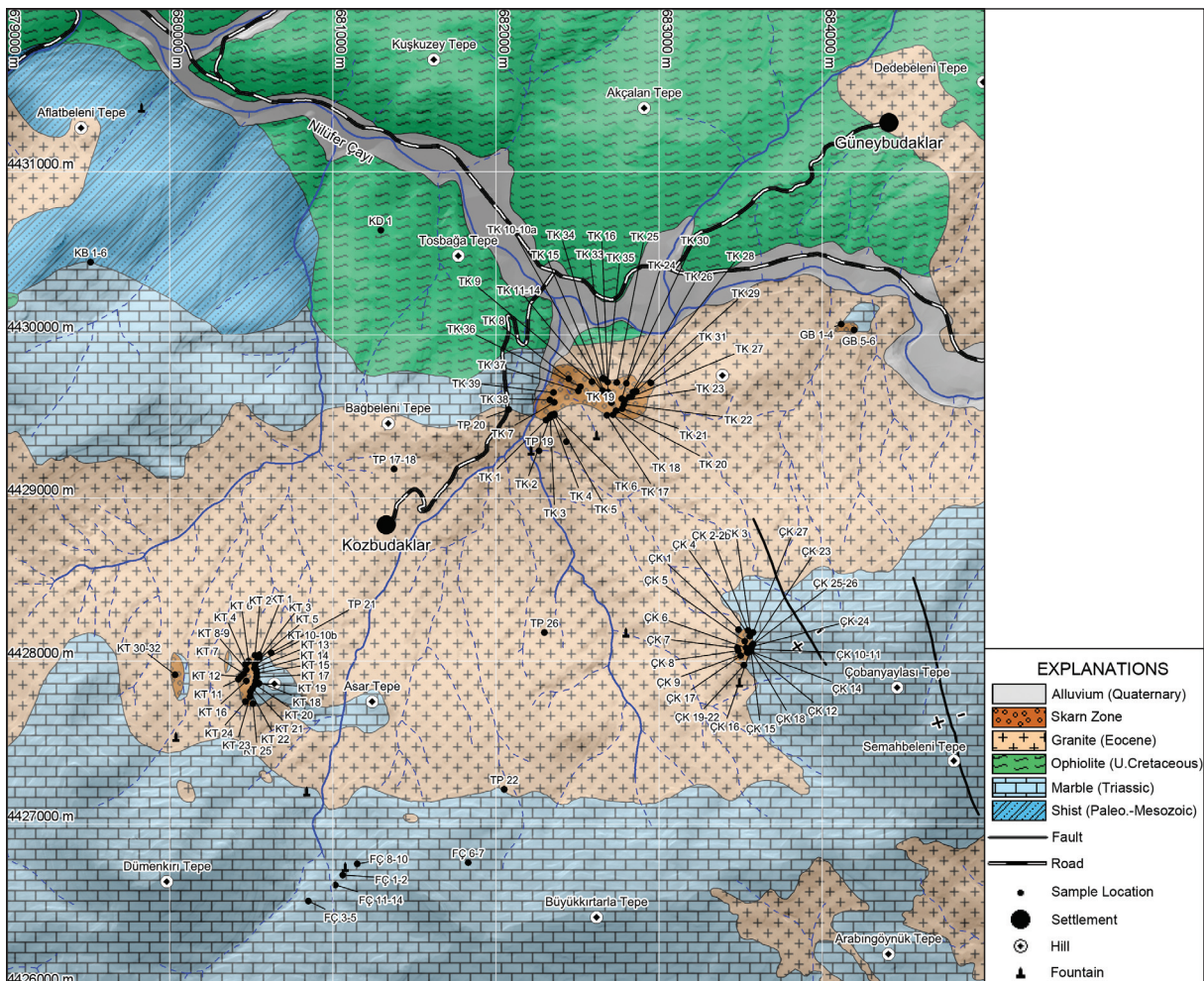


Table 1- Characteristics properties of skarn zones and sample numbers of skarn facies from the Kozbudaklar W-skarn deposit (after Orhan, 2017).

Rock type	Sample no	Skarn facies	Mineral assemblages	Characteristic properties
Endo-skarn	TK-1-6, 8, 9, 15, 16, 18, 19, 21, 29, 37, 39; KT-9, 11, 13, 15, 17, 18, 20, 23; GB-2, 4	Plg-Pyx skarn	Plg (Lab) + Pyx (Hd) + Q ± Sph ± Ap ± Bi ± Amp ± Ort ± Cc ± Prt ± Cpr ± Pr ± Mt ± Src	Coarse-to fine-grained, granular texture, occurs at the contact of the Topuk Pluton and composed of labradorite plagioclase (An ₅₅₋₆₄) and hedenbergitic (Hd ₉₅₋₉₆) clinopyroxene.
Exoskarn	TK-10/10a, TK-11, 13, 14, 22, 23, 26-28, 30, 33, 35	Pyx skarn	Pyx (Hd) ± Q ± Cc ± Sph ± Sch ± Prt ± Pr ± Mrc ± Lm	Occurs at the endoskarn contact, it has granoblastic texture and is composed dominantly (>95%) clinopyroxene (Hd ₉₃₋₉₄). Mo-content low scheelite is formed with hedenbergite and gives blue reflection color under ultraviolet light. Interstitial quartz and calcite are observed.
	TK-17, 20, 31, 38; KT-3 21, 22, 24, 25; ÇK-23, 25, 26; GB-3, 6, 7	Pyx-Gar skarn	Pyx (Hd-Di) + Gar (Grs) ± Wo ± Q ± Cc ± Sph ± Sch ± Chl	Develops as lenses within pyroxene zone and at the marble contact (distal zone). In proximal zone, garnet (Grs ₄₈₋₉₄) and clinopyroxene (Hd ₆₁₋₇₃) are accompanied by scheelite (Pov _{1,4}). In distal zone, wollastonite is observed with garnet (Grs ₆₅₋₉₅) and clinopyroxene (Hd ₁₇₋₂₂). Calcite and chlorite are the main alteration products and interstitial quartz and calcite are observed.
	ÇK-2/2b, 5, 7, 9, 17, 19-22; KT-5-8, 12, 14, 16, 31	Gar skarn	Gar (And) ± Pyx (Di) ± Ve ± Plg (An) ± Q ± Cc ± Sch ± Pr ± Cpr ± Mgt ± Chl ± Hm ± Cov	Composed of zoned garnet in proximal zone. Garnet composition varies from grossular to andradite (Grs ₂₄₋₉₂). Zoned garnet is replaced by vesuvianite and scheelite occurs in garnet rims. Mo-content in scheelite is high (Pov ₇₋₃₂) and gives yellow reflection color under ultraviolet light. Minor magnetite and sulfide mineralization are developed with secondary quartz, calcite and chlorite over the garnet. Skarn facies is cut by quartz and calcite veins.
	KT-10/10b, 19; ÇK-3, 4, 6, 8, 12, 16, 18, 25, 26	Gar-Pyx skarn	Gar (And) + Pyx (Di) ± Q ± Cc ± Ve ± Ep ± Plg ± Sch ± Pr ± Mgt ± Ap ± Chl	Zoned garnet is replaced by clinopyroxene, plagioclase (An ₉₁₋₉₇) inclusions are observed. Garnets represent composition between grossular and andradite (Grs ₃₀₋₉₀). Clinopyroxene is dominantly in diopside (Hd ₁₆₋₄₈) composition. Calcite and chlorite are the main alteration products. Pores and fractures of garnet are filled with quartz and calcite crystals.

Amp: amphibole; An: anorthite; And: andradite; Ap: apatite; Bio: biotite; Cc: calcite; Chl: chlorite; Cov: covellite; Cpr: chalcopyrite; Di: diopside; Ep: epidote; Gar: garnet; Hd: hedenbergite; Hm: hematite; Mgt: magnetite; Mrc: marcasite; Lab: labradorite; Lm: limonite; Ort: orthoclase; Pr: pyrite; Pyx: pyroxene; Prt: pyrrhotite; Q: quartz; Sep: scapolite; Sph: sphene; Src: sericite; Sch: scheelite; Ve: vesuvianite; Wo: wollastonite.

formed as replacement product of clinopyroxenes are mostly anhedral (Orhan, 2017). Clinopyroxenes in the proximal zone have hedenbergite (Hd₉₄₋₆₁) composition and those in distal zone have diopside composition (Hd₁₇₋₂₂). Garnets have composition varying from grossular to andradite (Grs₄₈₋₉₅) and Mo content of scheelites is relatively low (Pov_{1,4-6}) (Table 1). Gar (garnet) and Gar-Pyx (garnet-pyroxene) skarn which are represented by zoned garnets are formed at pluton contact (in proximal zone) at Çobanyaylası and Kepçe Hill locations. Zoned garnets show composition of grossular – andradite (Grs₂₄₋₉₂) from core to the rim (Table 1). Clinopyroxenes have replaced the zoned garnets (Orhan, 2017) and have composition mostly of diopside (Hd₁₆₋₄₈) (Table 1). Scheelites are formed at bands of zoned garnets or as monomineralic

occurrences between garnets and clinopyroxenes (Orhan, 2017). Mo content of scheelites in this zone is quite high (Pov₇₋₃₂) (Table 1).

According to Orhan (2017), hydrous products of retrograde stage such as epidote are rarely occurred. Orhan (2017) also stated that scheelite mineralization was developed in the prograde (proximal zone) at different phases (stage I and II) under varying oxidation conditions. During retrograde (stage III) stage, main alteration minerals of calcite, chlorite and quartz and trace amount of magnetite and sulfur minerals were formed. In the last stage (stage IV) of Kozbudaklar skarn deposit, skarn facies in the proximal zone are interrupted by barren quartz and calcite veins.

5. Geochemical Characteristics of Kozbudaklar Skarn Deposit

Mineral associations (described with mineralogical and petrographic analyses) and corresponding sample names of skarn facies in the Kozbudaklar skarn deposit are shown in table 1. Results of major oxide and trace element analyses for representative samples from skarn facies, Topuk Granodiorite and İnönü marble are given in table 2. Chemical analysis of Topuk Granodiorite (host rock of Kozbudaklar skarn deposit) is taken from Orhan et al. (2014a).

5.1. Major Element Geochemistry

The exoskarn zone is classified based on compositions of carbonate rock (magnesian or calcic composition) and skarn minerals (Burt, 1977; Einaudi et al., 1981). According to Orhan (2017), exoskarn zone and carbonate host rock in the region are of calcic character which is clearly visible from ACF triangular $[(Al_2O_3+Fe_2O_3)-(Na_2O+K_2O) - (CaO-3.3P_2O_5) - (MgO+MnO+FeO)]$ diagram (Figure 3) (Barton et al., 1991). In the diagram, exoskarn zone rocks (except for samples TK-22 and KT-3) are plotted in the field of calcium-silicate minerals (anorthite, garnet, vesuvianite, diopside and wollastonite/calcite). Samples of Pyx (TK-22) and Pyx-Gar skarn (KT-3) with high Al_2O_3 content are sampled from plutonic rock and locations close to the plagioclase-pyroxene skarn contact.

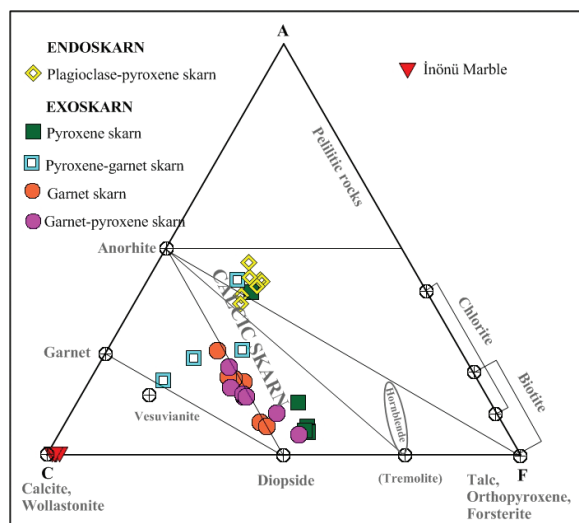


Figure 3- Positions of skarn zone samples in the ACF $[(Al_2O_3+Fe_2O_3)-(Na_2O+K_2O) - (CaO-3.3P_2O_5) - (MgO+MnO+FeO)]$ ternary diagram (Barton et al., 1991).

5.2. Geochemistry of Ore Elements

Mineral content of skarn deposits is quite variable. Geochemical studies on these deposits indicate the development of metal separation zones from proximal to distal zone and metal contents attain a significant economic size at the distal zone (Meinert et al., 2005). Metal contents of the Kozbudaklar skarn deposit are high particularly in the proximal zone. In addition to W, Cu concentration is partly high for two samples (208.1 and 247.8 ppm) in Plg-Pyx skarn (in endoskarn zone) at the Tepeköydedesi location (Table 2). W and Mo concentrations are increased in the exoskarn zone at Tepeköydedesi, Çobanyaylası and Kepçe Hill locations. W and Mo contents in Pyx and Pyx-Gar skarn are 433.7 to 5507 ppm (ave. 2330 ppm) and 7.8 to 90.2 ppm (ave. 40.28 ppm), respectively. Concentrations of these elements in the Gar and Gar-Pyx skarn (where zoned garnets are occurred) are higher ranging from 270.8 to 7615.5 ppm (2485.8 ppm) and from 6.7 to 492.5 ppm (ave. 106.6 ppm), respectively.

5.3. Rare Earth Element Geochemistry

Σ REE contents of Plg-Pyx and Pyx-Gar skarns at Kozbudaklar (except for samples with >400 ppm W) are recognized to be partly higher than those of granodiorite and metamorphic rocks (Tables 3). Σ REE contents are decreased from endoskarn zone (Plg-Pyx skarn) at the granitoid contact to the exoskarn zone. Σ REE contents of Topuk granodiorite, endoskarn, ekzoskarn zones and İnönü marble are 75.8 to 158.9 ppm (ave. 106.2 ppm), 75.8 to 171.5 ppm (ave. 114.6 ppm), 3.5 to 290.8 ppm (ave. 48.72 ppm) and 2.3 to 15.3 ppm (ave. 6.1 ppm) (Tables 2 - 3).

Σ REE contents of Topuk granodiorite are higher with respect to chondrite and light rare earth elements (LREE; 15 to 110-fold) are much more enriched than those of heavy rare earth elements (HREE; 10 to 20-fold) (Figure 4 - 8). $(La/Yb)_n$ $[(La/Yb)_n=(La/0.237)/(Yb/0.17)]$ (Sun and McDonough, 1989) ratio of samples is from 3.17 to 11.34 (ave. 6.35), LREE/HREE ratio ranges from 5.9 to 15.6 (ave. 9.1) and Eu/Eu^* $[Eu/Eu^*=(Eu/(Sm+Gd)*0.5)]$ ratio (Sun and McDonough, 1989) is in the range of 0.67 to 0.83 (ave. 0.76) (Tables 2 - 3). LREEs of Topuk granodiorite are greater than HREEs and show a slight convex pattern with a negative Eu anomaly.

The degree of enrichment of REEs for the İnönü marble is lower than that of chondrite. LREEs are

Table 2- Representative major oxide and trace element compositions of Topuk granodiorite, skarn facies and Inönü marble.

Sample no	TP-3	TP-10	TP-12	TP-18	TP-23	TK-1	TK-15	TK-13	KT-23	TK-17	TK-31	KT-3	KT-24	TK-10	TK-11	TK-13	TK-14	TK-22	
Rock type	TOPUK PLUTON										EXOSKARN ZONE								
Skarn facies											Pyroxene-garnet skarn								
Major oxide (%)	Plagioclase-pyroxene skarn										Pyroxene skarn								
SiO ₂	61.21	65.42	57.93	63.80	69.00	50.77	45.92	50.38	47.75	48.93	45.30	48.89	41.01	48.44	53.95	55.68	48.94	47.91	
TiO ₂	0.32	0.36	0.54	0.44	0.25	0.60	0.26	0.69	0.54	0.02	0.48	0.75	0.68	0.04	0.02	0.01	0.09	0.55	
Al ₂ O ₃	15.34	16.37	18.18	16.62	15.35	19.37	20.84	18.03	17.84	0.61	12.74	20.17	12.13	1.32	0.31	0.24	5.27	17.79	
Fe ₂ O ₃	4.10	4.64	7.39	5.04	3.08	7.07	10.07	7.56	8.43	24.55	11.74	6.66	8.61	25.72	23.66	22.80	21.02	10.22	
MnO	0.09	0.14	6.65	0.12	0.08	0.31					0.67	0.45	0.51	1.49	1.60	1.53	1.32	0.37	
MgO	1.25	1.37	0.22	1.62	1.06	2.86	1.48	2.61	2.75	3.07	3.12	2.19	2.40	1.82	1.34	1.27	2.37	1.50	
CaO	8.58	5.15	2.76	4.85	3.97	14.08	15.62	18.40	20.31	22.23	23.58	18.20	31.74	21.60	19.62	18.96	19.92	18.24	
Na ₂ O	3.17	3.38	7.03	3.49	3.14	2.81	1.66	1.15	0.92	0.07	0.43	1.26	0.01	0.22	0.07	0.06	0.73	0.03	
K ₂ O	1.67	1.79	3.43	2.52	3.22	0.14	0.98	0.05	0.07	<0.01	0.60	0.05	<0.01	0.18	<0.01	0.01	0.51	0.02	
P ₂ O ₅	0.12	0.14	1.38	0.13	0.08	0.16	0.10	0.14	0.23	0.04	0.13	0.17	0.06	0.06	0.04	0.05	0.10	0.19	
Cr ₂ O ₃	0.03	0.04	0.13	0.05	0.06	0.029	0.022	0.031	0.026	0.007	0.034	0.030	0.050	0.007	0.016	0.021	0.006	0.031	
A.Z.	4.00	1.00	0.04	1.10	0.50	1.7	2.4	0.3	0.5	1.2	0.9	1.0	2.6	1.0	1.1	1.4	0.4	3.0	
Total	99.88	99.80	0.80	99.78	99.80	99.85	99.84	99.82	99.87	99.85	99.77	99.80	99.85	99.92	99.54	99.20	99.87	99.84	
Trace elements (ppm)																			
W	<0.5	<0.5	<0.5	<0.5	<0.5	1.1	0.9	18.1	0.6	433.7	30.7	14.7	46.3	3.7	2944.5	5507.3	11.0	48.2	
Mo	0.20	<0.1	0.20	<0.1	0.60	1.0	46.2	1.0	0.6	7.8	1.4	0.7	5.0	1.9	55.3	90.2	0.6	1.0	
Cu	12.60	9.00	181.80	7.70	7.80	247.8	208.1	9.6	13.3	2.5	0.9	11.0	5.7	21.1	6.1	4.4	70.1	0.8	
Pb	1.00	2.00	2.00	2.70	5.80	2.3	5.7	2.1	1.7	0.7	1.9	2.1	1.7	1.8	0.8	1.2	1.8	1.4	
Zn	23.00	47.00	48.00	45.00	22.00	10	21	15	27	23	18	23	176	27	18	27	16	17	
Au (ppb)	<0.5	<0.5	1.00	<0.5	<0.5	<0.5	0.6	<0.5	<0.5	1.0	3.8	<0.5	1.6	<0.5	0.8	<0.5	2.6	3.7	
Rare earth elements (ppm)																			
La	20.00	16.70	16.60	39.20	14.50	11.0	40.4	31.3	22.0	0.9	74.0	36.7	14.6	2.7	0.4	0.7	11.4	17.4	
Ce	36.60	33.40	35.90	69.90	27.20	26.9	66.5	67.0	44.9	0.6	143.2	81.8	41.0	5.3	0.7	0.5	20.6	41.1	
Pr	4.21	4.13	5.05	7.11	3.47	3.67	7.70	8.46	5.28	0.16	13.62	9.11	5.65	0.60	0.14	0.18	2.05	4.97	
Nd	16.90	16.60	20.50	24.70	14.90	14.8	29.1	34.5	17.6	1.1	39.9	36.3	24.9	2.4	0.8	0.6	8.0	18.4	
Sm	20.00	3.58	4.69	3.86	2.86	3.49	3.84	6.99	2.95	0.16	5.22	7.10	5.53	0.34	0.15	0.22	1.06	4.41	
Eu	0.81	0.92	1.13	0.85	0.81	0.58	0.54	1.06	0.71	0.04	1.34	1.05	1.17	0.06	0.05	0.05	0.15	0.91	
Gd	2.76	3.52	4.5	3.75	3.06	3.68	3.32	6.33	2.60	0.16	4.42	6.43	5.03	0.46	0.20	0.34	1.05	4.71	
Tb	0.44	0.53	0.78	0.55	0.47	0.59	0.41	0.89	0.38	0.03	0.59	0.89	0.68	0.05	0.03	0.04	0.14	0.68	
Dy	2.78	3.24	5.20	3.20	3.29	3.89	2.70	5.82	2.50	0.22	3.51	5.52	4.06	0.44	0.22	0.18	0.92	4.60	

Table 2- continued

Sample no	TP-3	TP-10	TP-12	TP-18	TP-23	TK-1	TK-15	TK-13	KT-23	TK-17	TK-31	KT-3	KT-24	TK-10	TK-11	TK-13	TK-14	TK-22		
Rock type	TOPIUK PLUTON					ENDOSKARN ZONE					EXOSKARN ZONE					Pyroxene skarn				
Skarn facies						Plagioclase-pyroxene skarn					Pyroxene-garnet skarn									
Rare earth elements (ppm)																				
Ho	0.51	0.72	1.03	0.69	0.60	0.82	0.58	1.17	0.46	0.03	0.62	1.06	0.80	0.12	0.06	0.06	0.19	0.94		
Er	1.70	2.30	3.23	1.93	1.89	2.56	1.70	3.40	1.46	0.11	1.85	3.10	2.36	0.43	0.21	0.21	0.57	2.67		
Tm	0.27	0.38	0.50	0.32	0.31	0.39	0.26	0.52	0.20	0.03	0.27	0.49	0.32	0.10	0.04	0.04	0.11	0.41		
Yb	1.79	2.57	3.76	2.48	2.07	3.01	1.90	3.50	1.48	0.32	1.94	3.10	2.31	0.87	0.47	0.29	0.83	2.86		
Lu	0.31	0.40	0.58	0.38	0.33	0.44	0.35	0.57	0.18	0.06	0.30	0.47	0.33	0.15	0.10	0.05	0.19	0.49		
ΣREE	92.15	88.59	103.90	158.92	75.76	75.82	159.30	171.51	102.7	3.92	290.78	193.12	108.74	14.02	3.57	3.46	47.26	104.5		
ΣLREE	84.35	78.85	88.82	149.37	66.80	64.12	151.40	155.64	96.04	3.12	281.70	178.49	97.88	11.86	2.44	2.59	44.31	91.90		
ΣHREE	7.80	10.14	15.08	9.55	8.96	11.70	7.90	15.87	6.66	0.80	9.08	14.63	10.86	2.16	1.13	0.87	2.95	12.65		
LREE/HREE	10.8	7.8	5.9	15.6	7.5	5.5	19.2	9.8	14.4	3.9	31.0	12.2	9.0	5.49	2.2	3.0	15.0	7.26		
(La/Yb) _n	8.01	4.66	3.17	11.34	5.02	2.62	15.25	6.41	10.66	2.02	27.36	8.49	4.53	2.23	0.61	1.73	9.85	4.36		
Eu/Eu*	0.83	0.78	0.71	0.67	0.83	0.49	0.45	0.48	0.77	0.76	0.83	0.47	0.67	0.46	0.88	0.56	0.43	0.61		
Sample no	ÇK-2	ÇK-7	ÇK-9	ÇK-21	KT-12	KT-16	ÇK-4	ÇK-6	ÇK-12	ÇK-16	ÇK-26	KT-10b	KT-19	TK-24	KT-4	ÇK-14	ÇK-22	KB-7		
Rock type	EXOSKARN ZONE																			
Skarn facies	Garnet skarn																			
Major oxide (%)	Garnet-pyroxene skarn																			
SiO ₂	36.38	36.26	38.59	36.63	60.98	41.18	37.65	38.54	38.68	38.30	37.43	76.79	69.70	0.53	0.16	0.23	0.10	0.37		
TiO ₂	<0.01	<0.01	0.21	0.01	0.15	0.07	0.01	0.01	0.19	0.22	<0.01	0.02	<0.01	<0.01	<0.01	<0.01	<0.01	<0.01		
Al ₂ O ₃	2.22	9.23	13.33	1.46	5.48	8.82	7.79	11.02	6.28	6.70	6.36	1.29	0.31	0.07	0.05	<0.01	0.03	0.10		
Fe ₂ O ₃	25.71	14.85	11.57	27.04	11.95	18.03	15.80	13.11	18.28	18.96	19.94	7.91	11.61	0.16	0.05	0.06	0.08	0.05		
MnO	1.00	1.80	2.38	1.03	0.94	0.79	1.88	2.70	1.62	1.57	1.51	0.59	1.68	0.02	<0.01	0.01	<0.01	<0.01		
MgO	0.70	1.09	0.64	0.49	0.33	0.33	1.49	1.54	2.00	1.38	1.04	1.21	2.32	0.81	0.56	1.43	1.00	0.83		
CaO	30.92	29.67	29.46	30.08	18.27	29.42	30.43	29.56	29.33	30.17	30.59	9.74	12.74	55.35	55.77	55.07	55.43	55.29		
Na ₂ O	<0.01	<0.01	0.02	<0.01	0.08	<0.01	<0.01	0.02	0.02	0.01	<0.01	0.03	0.07	<0.01	<0.01	<0.01	<0.01	<0.01		
K ₂ O	<0.01	<0.01	0.01	<0.01	0.10	0.03	<0.01	<0.01	<0.01	<0.01	<0.01	<0.01	<0.01	0.02	<0.01	<0.01	<0.01	0.03		
P ₂ O ₅	0.03	0.03	0.02	0.02	0.04	0.02	0.04	0.05	0.05	0.04	0.04	0.06	0.05	<0.01	0.02	<0.01	<0.01	<0.01		
Cr ₂ O ₃	0.034	0.029	0.035	0.031	0.032	0.034	0.030	0.056	0.024	0.028	0.024	0.063	0.051	<0.002	<0.002	<0.002	<0.002	0.002		
A.Z.	2.8	6.5	3.7	3.0	1.6	1.2	4.3	3.3	3.4	2.5	2.8	1.4	0.4	43.0	43.4	43.2	43.3	43.3		
Total	99.84	99.49	99.92	99.80	99.93	99.93	99.40	99.91	99.89	99.89	99.74	99.10	98.91	99.96	99.97	99.96	99.96	99.97		

Table 2- continued

Sample no	ÇK-2	ÇK-7	ÇK-9	ÇK-21	KT-12	KT-16	ÇK-4	ÇK-6	ÇK-12	ÇK-16	ÇK-26	KT-10b	KT-19	TK-24	KT-4	ÇK-14	ÇK-22	KB-7	
Rock type	İNÖNÜ MARBLE																		
Skarn facies	Garnet-pyroxene skarn																		
Trace elements (ppm)	EXOSKARN ZONE																		
	Garnet skarn								Garnet-pyroxene skarn										
W	808.2	3411.5	86.3	1163.6	293.5	8.7	3853.9	38.6	107.9	270.8	1320.1	6013.4	7615.5	1.0	<0.5	<0.5	0.5	<0.5	
Mo	40.1	82.5	2.7	17.8	6.7	0.7	155.9	0.6	10.4	20.7	99.3	492.6	44.0	<0.1	<0.1	<0.1	<0.1	0.1	
Cu	1.4	1.0	1.2	0.8	2.6	15.0	1.4	1.2	1.1	1.0	0.8	2.9	1.6	5.5	1.9	1.4	2.6	0.9	
Pb	0.7	1.8	0.6	0.6	0.6	1.3	0.7	0.7	0.6	0.5	0.5	0.9	0.8	1.2	0.3	0.3	0.4	0.9	
Zn	11	32	43	17	17	38	32	26	36	32	8	19	29	1	2	2	2	1	
Au (ppb)	0.8	<0.5	<0.5	<0.5	0.6	1.8	0.6	<0.5	<0.5	<0.5	2.2	2.1	3.7	<0.5	<0.5	<0.5	<0.5	<0.5	
Rare earth elements (ppm)																			
La	1.6	0.3	0.8	1.8	1.9	1.0	0.9	0.6	2.1	2.4	1.0	0.8	0.9	4.4	1.8	1.4	0.7	0.8	
Ce	5.1	1.8	2.0	3.7	3.1	7.9	3.6	2.5	9.7	12.0	5.9	2.7	1.8	2.2	0.7	0.5	0.7	1.0	
Pr	0.79	0.54	0.45	0.38	0.69	2.25	0.91	0.82	1.67	2.08	0.97	0.40	0.21	0.87	0.24	0.20	0.11	0.16	
Nd	2.9	4.0	4.6	1.1	4.8	15.2	5.0	5.8	7.9	10.5	2.9	1.7	0.9	4.0	0.8	0.8	0.3	1.0	
Sm	0.27	0.58	1.76	0.20	1.49	2.92	0.37	0.72	1.78	2.27	0.22	0.28	<0.05	0.66	0.11	0.06	<0.05	0.11	
Eu	0.42	0.70	0.83	0.20	0.70	1.61	0.45	1.00	0.56	0.69	0.20	0.12	0.02	0.16	0.03	0.04	<0.02	0.04	
Gd	0.35	0.43	2.63	0.22	1.54	2.27	0.36	0.38	1.19	1.61	0.25	0.21	0.05	0.99	0.34	0.29	0.11	0.16	
Tb	0.04	0.03	0.36	0.02	0.17	0.27	0.05	0.04	0.13	0.15	0.03	0.03	<0.01	0.13	0.04	0.04	0.02	0.02	
Dy	0.28	0.19	2.65	0.18	1.17	1.70	0.38	0.37	0.52	0.77	0.27	0.18	<0.05	0.72	0.32	0.23	0.11	0.19	
Ho	0.06	0.05	0.66	0.04	0.17	0.34	0.07	0.05	0.10	0.11	0.04	0.03	<0.02	0.18	0.08	0.04	<0.02	0.04	
Er	0.11	0.11	2.04	0.11	0.44	1.11	0.12	0.19	0.27	0.24	0.14	0.07	<0.03	0.46	0.21	0.18	0.13	0.14	
Tm	0.03	0.02	0.29	0.01	0.08	0.17	0.02	0.03	0.04	0.05	0.02	0.01	<0.01	0.08	0.03	0.02	0.02	0.01	
Yb	0.21	0.18	1.76	0.07	0.49	1.06	0.17	0.14	0.20	0.33	0.12	0.09	<0.05	0.41	0.21	0.15	0.07	0.11	
Lu	0.03	0.03	0.27	0.01	0.06	0.15	0.03	0.01	0.04	0.05	0.02	0.02	<0.01	0.05	0.03	0.03	0.01	0.01	
ΣREE	12.19	8.96	21.10	8.04	16.80	37.95	12.43	12.65	26.20	33.25	12.08	6.64	3.81	15.31	4.94	3.98	2.28	3.79	
ΣLREE	11.43	8.35	13.07	7.60	14.22	33.15	11.59	11.82	24.90	31.55	11.44	6.21	3.81	13.28	4.02	3.29	1.92	3.27	
ΣHREE	0.76	0.61	8.03	0.44	2.58	4.80	0.84	0.83	1.30	1.70	0.64	0.43	-	2.03	0.92	0.69	0.36	0.52	
LREE/HREE	15.04	13.69	1.63	17.27	5.51	6.91	13.80	14.24	19.15	18.56	17.88	14.44	-	6.54	4.37	4.77	5.33	6.29	
(La/Yb)n	5.47	1.20	0.33	18.44	2.78	0.68	3.80	3.07	7.53	5.22	5.98	6.38	-	7.70	6.15	6.69	7.17	5.22	
Eu/Eu*	4.18	4.10	1.18	2.90	1.40	1.84	3.72	5.26	1.11	1.05	2.60	1.45	-	0.60	0.44	0.76	-	0.92	

Table 3- ΣREE concentrations and LREE/HREE, (La/Yb)_n, Eu/Eu* ratios of Topuk granodiorite, skarn facies and İnönü marble and scheelite-containing samples.

ROCKS	ΣREE(ppm)	ΣLREE(ppm)	ΣHREE(ppm)	LREE/HREE	(La/Yb) _n	Eu/Eu*
<i>TOPUK PLUTON</i>	75.8-158.9 (mean 106.2)	66.8-149.4 (mean 95.4)	7.8-15.1 (mean 10.7)	5.9-15.6 (mean 9.1)	3.17-11.34 (mean 6.35)	0.67-0.83 (mean 0.76)
<i>ENDOSKARN ZONE</i>						
Plg-Pyx skarn	75.8-171.5 (mean 114.6)	64.1-155.6 (mean 103.7)	6.7-15.9 (mean 10.9)	5.5-19.2 (mean 10.4)	2.62-15.25 (mean 10.17)	0.45-0.84 (mean 0.77)
<i>EXOSKARN ZONE</i>						
Pyx-Gar skarn	108.7-290.8 (mean 183.0)	97.9-281.7 (mean 171.9)	9.1-14.6 (mean 11.1)	9.0-31.0 (mean 16.3)	4.53-27.36 (mean 12.63)	0.47-0.83 (mean 0.63)
<i>Scheelite-containing samples</i>	3.9	3.1	0.8	3.9	2.02	0.76
Pyx skarn	14.0-104.6 (mean 55.3)	11.9-91.9 (mean 49.4)	2.2-12.7 (mean 5.9)	5.5-15.0 (mean 9.3)	2.23-9.85 (mean 5.48)	0.43-0.61 (mean 0.50)
<i>Scheelite-containing samples</i>	3.5-3.6 (mean 3.5)	2.4-2.6 (mean 2.5)	0.87-1.13 (mean 1.00)	2.2-2.9 (mean 2.6)	0.61-1.73 (mean 1.17)	0.56-0.88 (mean 0.72)
Gar skarn	16.8-38.0 (mean 25.3)	13.1-33.2 (mean 20.2)	2.6-8.0 (mean 5.1)	1.6-6.9 (mean 4.7)	0.33-2.78 (mean 1.26)	1.18-1.84 (mean 1.47)
<i>Scheelite-containing samples</i>	8.0-12.2 (mean 9.7)	7.6-11.4 (mean 9.1)	0.4-0.8 (mean 0.6)	13.7-17.3 (mean 15.3)	1.20-18.44 (mean 8.37)	2.90-4.18 (mean 3.73)
Gar-Pyx skarn	12.7-33.3 (mean 24.0)	11.8-31.6 (mean 22.8)	0.8-1.7 (mean 1.3)	14.2-19.6 (mean 17.3)	3.07-7.53 (mean 5.27)	1.05-5.26 (mean 2.47)
<i>Scheelite-containing samples</i>	3.8-12.4 (mean 8.7)	3.8-11.6 (mean 8.3)	0.4-0.8 (mean 0.5)	13.8-17.9 (mean 11.5)	3.80-6.38 (mean 4.04)	1.45-3.72 (mean 1.94)
<i>İNÖNÜ MARBLE</i>	2.3-15.3 (mean 6.1)	1.9-12.3 (mean 5.2)	0.4-2.0 (mean 0.9)	4.4-6.5 (mean 5.5)	5.22-7.70 (mean 6.57)	0.44-0.92 (mean 0.55)

enriched 0.3 to 15-fold whilst HREEs are enriched only 0.3 to 2-fold (Figure 4-8). Regarding marble, (La/Yb)_n ratio is in the range of 5.22 to 7.70 (ave. 6.57), LREE/HREE ratio is between 4.4 and 6.5 (ave. 5.5 ppm) and (Eu/Eu*)_n ratio (except for sample ÇK-22) varies from 0.44 to 0.92 (Tables 2 - 3). Eu (<0.02 ppm) and Sm (<0.05 ppm) concentrations of sample ÇK-22 are quite low. According to these results, LREE and HREE contents of marbles show flat patterns with variable Eu anomaly. REE trends of marbles display a significant negative Ce anomaly indicating deposition in marine environment (Murray et al., 1990).

Regarding Plg-Pyx skarn samples collected from granitoid contact, LREEs and HREEs have been enriched 10 to 115-fold and 10 to 15-fold with respect to chondrite (Figure 4). LREE enrichment is slightly higher than granodiorite. For the endoskarn zone (La/Yb)_n ratio is in the range of 2.62 to 15.25 (ave. 10.17), LREE/HREE ratio is between 5.5 and 19.2 (ave. 10.4) and (Eu/Eu*)_n ratio varies from 0.45 to 0.84 (ave. 0.77) (Tables 2 - 3). According to these results, like the Topuk granodiorite, the endoskarn zone is enriched by LREE and depleted in Eu.

Regarding Pyx-Gar skarn samples with low tungsten content, LREEs and HREEs have been enriched 10 to 200-fold and 15 to 20-fold with respect to chondrite (Figure 5). In one sample with relatively high tungsten concentration (TK-17) REEs are quite low; LREEs and HREEs have been enriched 0.5 to 3-fold and 0.5 to 2-fold. LREEs of samples with low tungsten content from Pyx-Gar skarn are much enriched than Topuk granodiorite. (La/Yb)_n, LREE/HREE and (Eu/Eu*)_n ratios of these samples are 4.53 to 27.36 (ave. 12.63), 9.0 to 31.0 (ave. 16.3) and 0.47 to 0.83 (ave. 0.63), respectively (Tables 2 - 3). These samples are represented by REE patterns similar to Topuk granodiorite – enriched LREE and depleted Eu trends (Figure 5). For the sample with relatively high tungsten content, (La/Yb)_n, LREE/HREE and (Eu/Eu*)_n ratios are found 2.02, 3.9 and 0.76. This sample shows depletion for Ce (consistent with marbles) and Eu and a flat pattern for LREE-HREE (consistent with Topuk granodiorite). Different from granodiorite and carbonate rocks, the same sample displays a relative enrichment for Tm, Yb and Lu.

ΣREE contents of samples from the Pyx skarn facies (except for sample TK-22) are slightly depleted

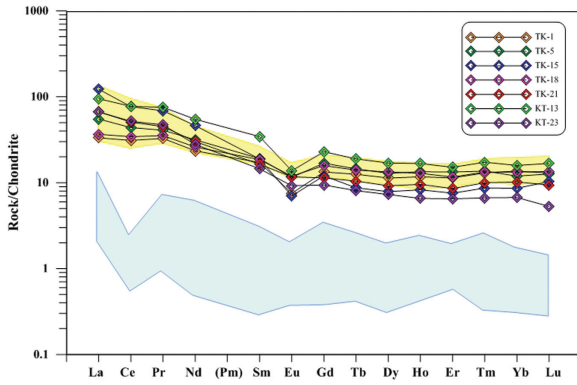


Figure 4- Rare earth element diagram for plagioclase-pyroxene skarn (endoskarn zone), Topuk pluton and İnönü marble (chondrite normalized values are from Nakamura, 1974) (yellow and blue shaded areas belong to Topuk pluton and İnönü marble).

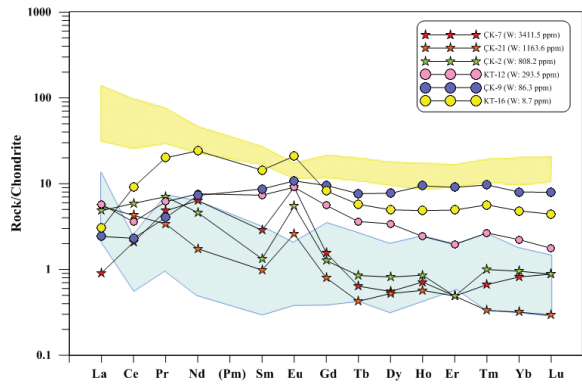


Figure 7- Rare earth element diagram for garnet skarn (exoskarn zone), Topuk pluton and İnönü marble (chondrite normalized values are from Nakamura, 1974) (yellow and blue shaded areas belong to Topuk pluton and İnönü marble).

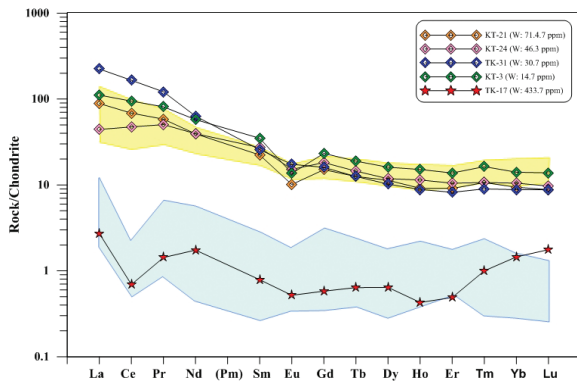


Figure 5- Rare earth element diagram for pyroxene-garnet skarn (exoskarn zone), Topuk pluton and İnönü marble (chondrite normalized values are from Nakamura, 1974) (yellow and blue shaded areas belong to Topuk pluton and İnönü marble).

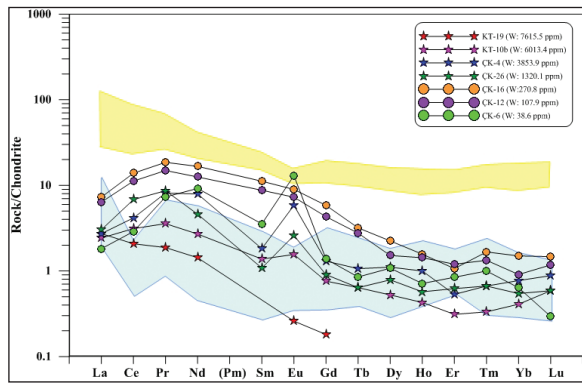


Figure 8- Rare earth element diagram for garnet-pyroxene skarn (exoskarn zone), Topuk pluton and İnönü marble (chondrite normalized values are from Nakamura, 1974) (yellow and blue shaded areas belong to Topuk pluton and İnönü marble).

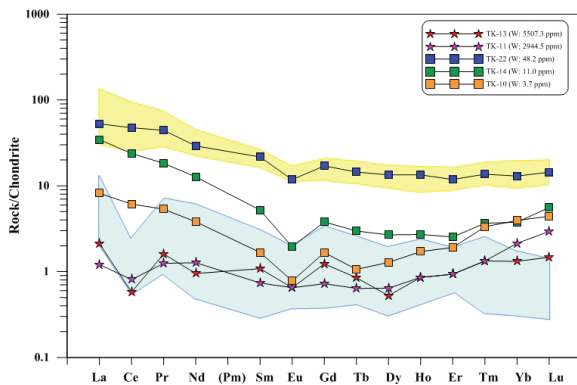


Figure 6- Rare earth element diagram for pyroxene skarn (exoskarn zone), Topuk pluton and İnönü marble (chondrite normalized values are from Nakamura, 1974) (yellow and blue shaded areas belong to Topuk pluton and İnönü marble).

with respect to Topuk granodiorite (Tables 2 - 3; Figure 6). However, their Tm, Yb and Lu concentrations are partly higher than those of granodiorite and carbonate rocks. Samples with low tungsten content (TK-10, TK-14 and TK-22) are represented by (La/Yb)_n, LREE/HREE and (Eu/Eu*)_n ratios of 2.23 to 9.85 (ave. 5.48), 5.5 to 15.0 (ave. 9.3) and 0.43 to 0.61 (ave. 0.50) and resemble Topuk granodiorite with their enriched LREE pattern and negative Eu anomaly. With increasing W content, ΣREE and Ce concentrations are significantly decreased (Figure 6). Samples with low W content are similar to İnönü marble with their low ΣREE content, negative Ce anomaly and flat-like pattern of LREE and HREEs and their negative Eu trend is consistent with granodioritic rocks (Figure 6). For these samples (La/Yb)_n is 0.61 to 1.73 (ave. 1.17), LREE/HREE is 2.2 to 2.9 (ave. 2.6) and (Eu/Eu*)_n is 0.56 to 0.88 (ave. 0.72) (Tables 2 - 3).

In Gar and Gar-Pyx skarn where zoned garnets are formed Σ REE contents are significantly lower than those of Topuk granodiorite (Tables 2 - 3; Figures 7 - 8). Samples with dominant andradite composition that formed via fluid infiltration are characteristic with convex LREE pattern, high Pr and Nd concentrations and positive Eu anomaly (Whitney and Olmsted, 1998). Σ REE contents of W-enriched samples from Gar skarn (8.0 to 12.2 ppm, ave. 9.7 ppm) are lower than those of W-poor samples (16.8 to 38.0 ppm, ave. 25.3 ppm) (Tables 2 - 3). Both type samples display positive Eu anomaly (Figure 7). Samples with low W content are represented by convex LREE trend and enriched HREE patterns. For these samples, (La/Yb)_n is 0.33 to 2.78 (ave. 1.26), LREE/HREE ratio is 1.6 to 6.9 (ave. 4.7) and (Eu/Eu*)_n ratio is 1.18 to 1.84 (ave. 1.47). For W-enriched samples, (La/Yb)_n is 1.20 to 18.44 (ave. 8.37), LREE/HREE ratio is 13.7 to 17.7 (ave. 15.3) and (Eu/Eu*)_n ratio is 2.90 to 4.18 (ave. 3.73). These samples with partly enriched LREE contents resemble the Topuk granodiorite and with HREE trends resemble the İnönü marble (Table 3; Figure 7).

Σ REE contents of Gar-Pyx skarn samples are lower than Topuk granodiorite (3.8 to 33.3 ppm, ave. 15.29 ppm) (Tables 2 - 3; Figure 8). With increasing W concentration Σ REE content is definitively decreased. Sample KT-19 with W concentration (7615.5 ppm) higher than other samples have quite low Eu and HREE contents (Tables 2 - 3; Figure 8). For other samples, (La/Yb)_n is 3.07 to 7.53, LREE/HREE ratio is 14.2 to 19.6 and (Eu/Eu*)_n is 1.05 to 5.26. Samples are characterized by convex LREE pattern, positive Ce, Pr, Nd and Eu anomalies and HREE trends similar to carbonate rocks.

6. Discussion and Results

Like other worldwide W-skarn deposits (Einaudi et al., 1981) the Kozbudaklar exoskarn zone is of calcic character with respect to major oxide content. This is consistent with mineralogical observations reported by Orhan (2017). The scheelite mineralization at Kozbudaklar occurs only in proximal zone of exoskarn zone. W and Mo concentrations are increased from Pyx and Pyx-Gar skarn (W: 433.7 to 5507 ppm, ave. 2330 ppm; Mo: 7.8 to 90.2 ppm, ave. 40.28 ppm) to Gar and Gar-Pyx skarn (W: 270.8 to 7615.5 ppm, ave. 2485.8 ppm; Mo: 6.7 to 492.5 ppm, ave. 106.6 ppm). Petrographic and mineral chemistry studies led Orhan (2017) to suggest that Pyx and Pyx-Gar skarn

were formed at the first phase of prograde stage and WO₃ and MoO₃ contents of scheelite in these skarn zones were found 76.95 to 78.3% and 0.35 to 1.42%, respectively. Scheelites in zoned garnets (Gar and Gar-Pyx skarn) which represent the second phase of prograde stage WO₃ MoO₃ in the range of 72.13 to 73.5% and 1.75 to 10.27% indicating a slight increase for Mo concentration.

Studies carried out on W-skarn deposits showed that due to circulation of hydrous fluids scheelite is sweep out towards the marble contact and scheelite grade is increased in the distal zone with the increase of hydrous mineral content and Ca ion activity (Kwak and Tan, 1981; Newberry, 1982; Zaw and Singoyi, 2000). By the mobilizing of Mo-enriched scheelites with meteoric water flux, pure scheelite and molybdenite are redeposited in association with hydrous minerals and quartz veins (Newberry, 1982). At Kozbudaklar skarn deposit, increase in Mo concentration cannot be attributed to molybdenite deposition indeed it is sourced from scheelite composition. According to Kwak and Tan (1981), scheelite forming in zoned garnet bands is not dissolved in some cases and therefore does not attain an economic size during the retrograde stage. At Kozbudaklar, increase in W and Mo contents indicates that oxidation conditions were changed during the fractionation of pluton (Newberry, 1998) which prevented scheelite to reach at a mineable grade.

The Topuk granodiorite hosting the scheelite mineralization is represented by an enriched LREE pattern and slight negative Eu anomaly (Eu/Eu* = 0.67 to 0.83). The İnönü marble, however, shows more flat LREE trend and negative Ce and variable Eu anomalies.

The Kozbudaklar deposit shows two different REE patterns through the skarn formation process. In addition to diverse rare earth element trends representing two different stages, Σ REE concentrations and Eu/Eu* ratios are also variable (Table 3). At Kozbudaklar, during the first phase of prograde stage (Plg-Pyx, Pyx-Gar and Pyx skarn), REE contents and Eu/Eu* (0.43 to 0.84) of samples with low tungsten concentration are quite consistent with Topuk granodiorite (Figures 4-5-6; Table 3). In the first stage when high-temperature early magmatic fluids were mobilized, Σ REE concentrations are found to be partly higher than granodiorite. In this facies where LREEs are enriched, LREE/HREE and (La/Yb)

n ratios are 5.5 to 31.0 and 2.23 to 27.36, respectively. In the second phase of prograde stage Σ LREE tend to be decreased (Table 3; Figure 9). Gar and Gar-Pyx skarn facies are characterized by positive Pr and Nd patterns, high Eu/Eu^* (1.05 to 5.26) and low $(La/Yb)_n$ ratios (0.33 to 7.53). In the progressive phase of prograde stage, LREE concentrations of the host rock were significantly depleted (by the fractionation of Topuk granitoid). High Eu/Eu^* anomaly implies mobilization of high-temperature fluids and changes in oxidation conditions in the second stage (Bau, 1991; Whitney and Olmsted, 1998; Bi et al., 2004; Oyman et al., 2013).

Samples with high scheelite contents also exhibit two different REE patterns. Scheelite-enriched samples show variable Ce and Eu anomalies. Mo-poor scheelites that formed in the first phase of prograde stage display flat-like LREE pattern and negative Ce anomaly resembling the İnönü marble and their Eu/Eu^* values (0.56 to 0.88) are similar to Topuk granodiorite (Figures 5-6; Table 3). LREE/HREE (2.2 to 3.9) and $(La/Yb)_n$ (0.61 to 2.02) ratios are considerably low. Mo-enriched scheelites of the second stage are represented by HREE trend conformable with the marbles and positive Ce and Eu anomalies (Figures 7 - 8; Table 3). Their LREE/HREE and $(La/Yb)_n$ ratios are 13.7 to 17.9 and 1.20 to 18.44, respectively. LREE/HREE ratios of Mo-enriched scheelites are greater than those of Mo-poor scheelites. However, it is clear that as the W concentration of samples is increased Σ REE concentrations are decreased (Figure

10). It was also observed in Moroccan tungsten skarn deposits where W concentrations are increased with decreasing Σ REE concentrations (Giuliani et al., 1987). Giuliani et al. (1987) found that $(La/Yb)_n$ and Eu/Eu^* of tungsten are extremely low when W concentrations (>1000 ppm) attain an economical potential and concluded that scheelite was not affected by the metamorphism and fluid-rock interaction under hydrothermal alteration conditions, in other words it behaved immobile. Considering low Eu/Eu^* ratios, they proposed reducing conditions for the scheelite formation and crystal formation was completed long before the interaction process.

It can be said that scheelite mineralization with low Σ REE contents that represents different stages of the Kozbudaklar skarn deposit was not affected by metamorphism and fluid-rock interaction under hydrothermal conditions. However, with increasing W concentration Eu/Eu^* ratios are found to increased (Figure 11a). Likewise Mo concentrations of the same samples are also increased (Figure 11b). Since Eu can replace Ca in scheelite, using positive or negative Eu anomalies redox conditions of ore-forming fluids may be estimated (Ghaderi et al., 1999). Negative Eu ($Eu/Eu^*=0.56$ to 0.88) anomaly recorded at Kozbudaklar may indicate partly reducing conditions for the formation of first-stage scheelites (Giuliani et al., 1987). However, increasing Mo concentration of scheelites (ave. 40.28 ppm \rightarrow ave. 106.6 ppm) might show oxidized conditions for scheelite-mineralizing fluids (Ghaderi et al., 1999). Song et

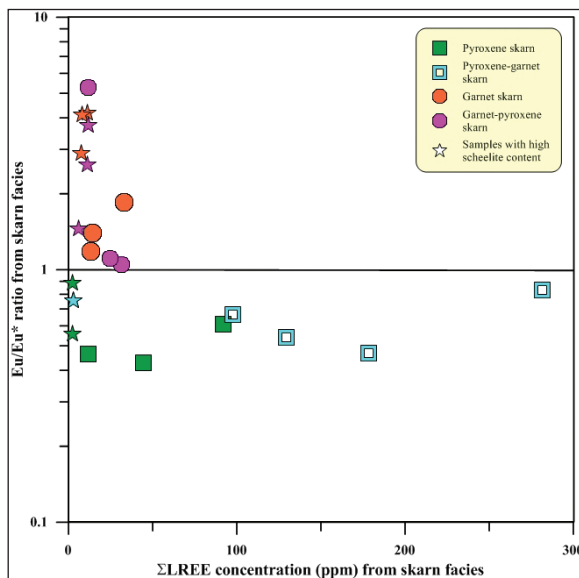


Figure 9- Eu/Eu^* ratios and Σ LREE concentrations of skarn zone samples.

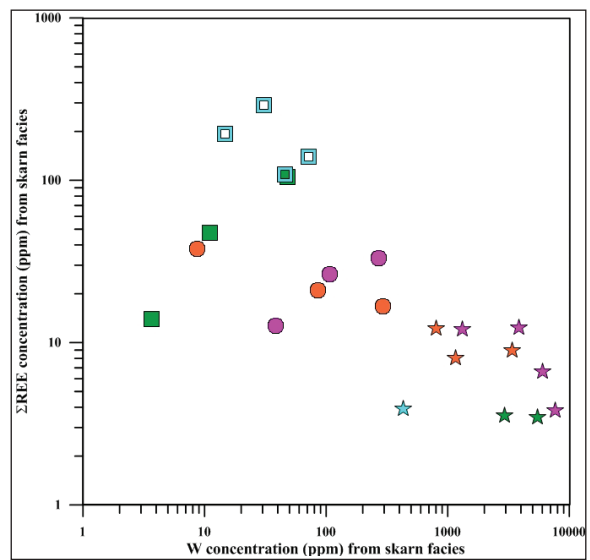


Figure 10- Σ REE and W concentrations of exoskarn zone samples (symbols as in figure 9).

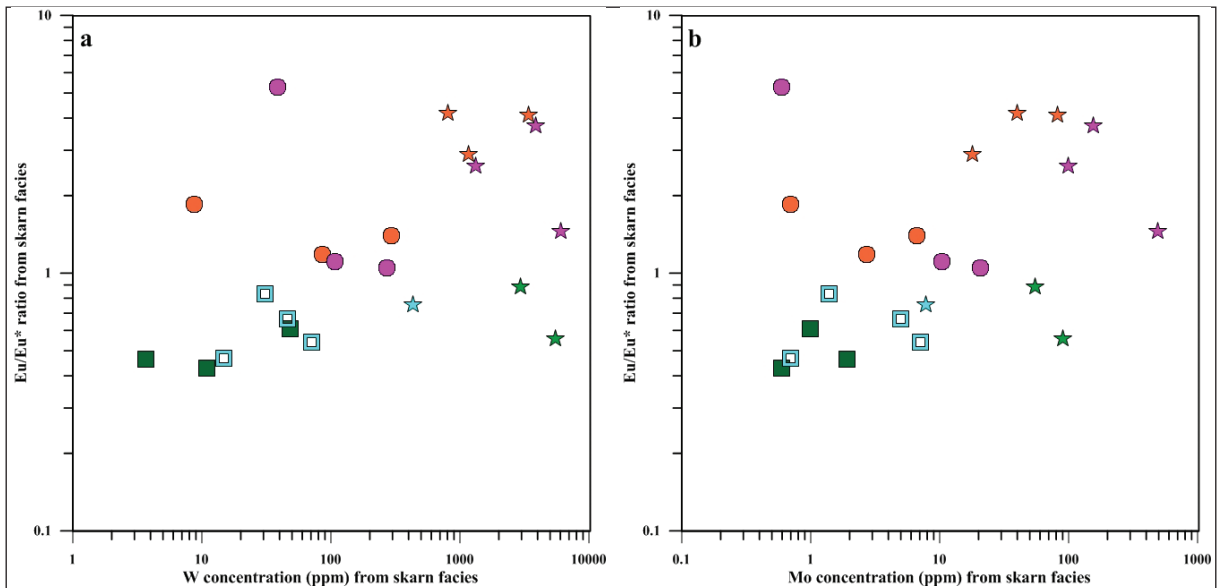


Figure 11- a) W and b) Mo concentrations and Eu/Eu* ratios of exoskarn zone samples (symbols as in figure 9).

al. (2014) also pointed out that Mo concentration increases and maximum Eu anomaly exists under oxidizing conditions. However, it has been shown that under reducing conditions Mo content of scheelite is lowered which gives rise to formation of molybdenite. Orhan (2017) defined different reducing conditions for scheelites which deposited at different phases in the Kozbudaklar skarn deposit. The presence of calc-silicate minerals (due to their ferrous composition) (e.g. garnet, pyroxene) recognized in association with the first-phase scheelites led to Orhan (2017) to suggest that scheelite was deposited under moderately reducing/moderately oxidizing conditions whilst Mo-enriched scheelites were crystallized under much oxidizing conditions after the boiling. Decreases in Σ LREE and increases in W and Mo contents and Eu/Eu* ratios support that second-phase scheelite mineralization took place during the fractionation of granitoid at much oxidizing conditions.

Acknowledgement

This study was supported by the Scientific and Technological Research Council of Turkey under grand no YDABAG-111Y289. Authors thank to Dr. Mehmet Demirbilek and Dr. Ahmet Orhan for their help during field works. We are grateful for constructive review by Dr. Özcan Dumanlılar and two anonymous reviewers, which improved the manuscript.

References

- Altunkaynak, Ş. 2007. Collision-driven slab break off magmatism in Northwestern Anatolia, Turkey. *Journal of Geology* 115, 63-82.
- Barton, M.D., Ilchik, R.P., Marikos, M.A. 1991. Metasomatizm. *Reviews in Mineralogy and Geochemistry* 26, 321-349.
- Bau, M. 1991. Rare-earth element mobility during hydrothermal and metamorphic fluid-rock interaction and the significance of the oxidation state of europium. *Chemical Geology* 93, 219-230.
- Bi, X., Hu, R., Cornell, D.H. 2004. The alkaline porphyry associated Yaoan gold deposit, Yunan, China: Rare earth element and stable isotope evidence for magmatic-hydrothermal ore formation. *Mineralium Deposita* 39, 21-20.
- Bingöl, E., Delaloye, M., Ataman, G. 1982. Granitic intrusion in Western Anatolia: a contribution to the geodynamic study of this area. *Ecloga Geologica Helvetica* 75 (2), 437-446.
- Brown, P.E., Bowman, J.R., Kelly, W. C. 1985. Petrologic and stable isotope constraints on source and evolution of skarn-forming fluids at Pine Creek, California. *Economic Geology* 80, 72-95.
- Burt, M.D. 1977. Mineralogy and petrology of skarn deposits. *Societa Italiana di Mineralogia e Petrologia* 33(2), 859-873.

- Delaloye, M., Bingöl, E. 2000. Granitoids from Western and Northwestern Anatolia: Geochemistry and modeling of geodynamic evolution. *International Geological Review* 42, 241-268.
- Einaudi, M.T., Meinert, L.D., Newberry, R.J. 1981. Skarn Deposits. *Economic Geology* 75, 317-391.
- Emre, H. 1996. Orhaneli Ofiyolitinin jeolojisi ve petrolojisi. Doktora Tezi, İstanbul Üniversitesi Fen Bilimleri Enstitüsü, İstanbul, 165 s. (unpublished).
- Fonteilles, M., Soler, P., Demange, M., Derre, C., Krier-Schellen, A.D., Verkaeren, J., Guy, B., Zahm, A. 1989. The scheelite skarn deposit of Salau (Ariege, French Pyrenees). *Economic Geology* 84, 1172-1209.
- Gerstner, M.R., Bowman, J.R., Parteris, J.D. 1989. Skarn formation at the Macmillan Pass Tungsten Deposit (Mactung), Yukon and Northwest Territories. I. P-T-X-V characterization of the methane-bearing skarn forming fluids. *The Canadian Mineralogist* 27, 545-563.
- Ghaderi, M., Palin, M.J., Sylvester, P.J., Campbell, I.H. 1999. Rare earth element systematics in scheelites from hydrothermal gold deposits in the Kalgoorlie-Norseman Region, Western Australia. *Economic Geology* 94, 423-437.
- Giuliani, G., Cheilletz, A., Mechiche, M. 1987. Behavior of REE during thermal metamorphism and hydrothermal infiltration associated with skarn and vein-type tungsten ore bodies in Central Morocco. *Chemical Geology* 64, 279-294.
- Harris, N.B.W., Kelley, S., Aral, I.O. 1994. Post-collision magmatism and tectonics in northwest Anatolia. *Contributions to Mineralogy and Petrology* 117, 241-252.
- Kwak, T.A.P., Tan, T.H. 1981. The geochemistry of zoning in skarn minerals at the King Island (Dolphin) mine. *Economic Geology* 76, 468-497.
- Lisenbee, A.A. 1972. Structural setting of the Orhaneli Ultramafic Massif near Bursa. Ph.D Thesis, University of State, Pennsylvania, USA, 170 pp. (unpublished).
- Lottermoser, B.G. 1992. Rare earth elements and hydrothermal ore formation processes. *Ore Geology Reviews* 7, 25-41.
- Meinert, L.D., Dipple, G.M., Nicolescu, S. 2005. World Skarn Deposits. Society of Economic Geologist, Inc. *Economic Geology* 100th Anniversary volume, 299-336.
- Michard, A. 1989. Rare earth element systematics in hydrothermal fluids. *Geochimica et Cosmochimica Acta* 53, 745-750.
- MTA. 1965. Türkiye Volfram ve Molibden Yatakları, Maden Tetkik ve Arama Genel Müdürlüğü Rapor No: 128, Ankara (unpublished).
- MTA. 1973. 1/25.000 ölçekli jeoloji haritası, H22d4, H22d3, İ21b2, İ22a1, İ22a2 Paftaları. Maden Tetkik ve Arama Genel Müdürlüğü, Ankara.
- MTA. 2002. 1/500.000 ölçekli Türkiye Jeoloji Haritası, İstanbul ve İzmir Paftaları. Maden Tetkik ve Arama Genel Müdürlüğü, Ankara.
- Murray, R.W., Buchholtz, T., Brink, M.R., Jones, D.L., Gerlach, D.C., Russ, G.P. 1990. Rare Earth Elements as Indicators of Different Marine Depositional Environments in Chert and Shale. *Geology* 18, 268-272.
- Nakamura, N. 1974. Determination of REE, Ba, Mg, Na and K in carbonaceous and ordinary chondrites. *Geochimica et Cosmochimica Acta* 38, 757-775.
- Newberry, R.J. 1982. Tungsten-bearing skarns of the Sierra Nevada. I, the Pine Creek mine, California. *Economic Geology* 77, 823-844.
- Newberry, R.J. 1998. W-and Sn-Skarn deposits, Lentz, D.R. (Ed.). Mineralized intrusion-related skarn systems. Mineralogical Association of Canada Short Course Series 26, 289-335.
- Okay, A.I. 1985. Kuzeybatı Anadolu'da yer alan metamorfik kuşaklar. *Ketin Sempozyumu Türkiye Jeoloji Kurultayı yayınları*, 83-93.
- Okay, A.I. 2004. Tectonics and high pressure metamorphism in northwest Turkey, Field trip guide book-P01. 32th International Geological Congress, APAT, Italy, 56 pp.
- Okay, A.I. 2011. Tavşanlı Zonu: Anatolid-Torid Bloku'nun dalma-batmaya uğramış kuzey ucu. *Maden Tetkik ve Arama Dergisi* 142, 195-226.
- Okay, A.I., Kelley, S.P. 1994. Tectonic setting, petrology and geochronology of jadeite + glaucophane and chloritoid + glaucophane schists from northwest Turkey. *Journal of Metamorphic Geology* 12, 455-466.
- Okay, A.I., Harris, N.B.W., Kelley, S.P., 1998. Exhumation of blueschists along a Tethyan suture in northwest Turkey. *Tectonophysics* 285, 275-299.
- Okay, A.I., Satır, M. 2006, Geochronology of Eocene plutonism and metamorphism in northwest Turkey: evidence for a possible magmatic arc. *Geodinamica Acta* 19, 251-266.
- Orhan, A. 2017. Evolution of the Mo-rich scheelite skarn mineralization at Kozbudaklar, Western Anatolia, Turkey: Evidence from mineral chemistry and fluid inclusion. *Ore Geology Reviews* 80, 141-165.

- Orhan, A., Demirbilek, M., Mutlu, H. 2014a. Mineral and whole-rock chemistry of the Topuk Granitoid (Bursa, Western Anatolia, Turkey). EGU General Assembly, Geophysical Research Abstracts, v.16.
- Orhan, A., Mutlu, H., Demirbilek, M. 2014b. Kozbudaklar (Bursa, Batı Anadolu) Şeelit Skarn Yatağının Mineralojik ve Jeokimyasal Karakteristikleri. 67. Türkiye Jeoloji Kurultayı, 14-18 Nisan, Ankara, 516-517.
- Orhan, A., Mutlu, H. 2015. Topuk Plütunu ile İlişkili Şeelit Skarn Yatağının (Bursa, Batı Anadolu) Evrimi ve Hidrotermal Akışkanların Kökeni. 68. Türkiye Jeoloji Kurultayı, 6-10 Nisan, Ankara, 336-339.
- Orhan, A., Mutlu, H., Demirbilek, M. 2015. Topuk Plütunu ile ilişkili skarn yataklarının (Bursa, Batı Anadolu) mineralojik, jeokimyasal ve kökenselel incelenmesi. Türkiye Bilimsel ve Teknolojik Araştırma Kurumu Proje No: 111Y289, 212 s. (unpublished).
- Oyman, T., Özgenç, İ., Tokcaer, M., Akbulut, M. 2013. Petrology, geochemistry and evolution of the iron skarns along the northern contact of the Eğrigöz Plutonic complex, Western Anatolia, Turkey. Turkish Journal of Earth Science 22, 61-97.
- Örgün, Y. 1993. Topuk-Göynükbelen (Orhaneli-Bursa) Yöresi Nikel Oluşumlarının Kökenselel İncelenmesi. Doktora Tezi, İTÜ Fen Bilimleri Enstitüsü, İstanbul, 216 s. (unpublished).
- Pehlivan, A.N. 1987. Kuzeybatı Anadolu wolfram ağırlıklı polimetal arama projesi (Kavap Rapor No:1) Bursa-İnegöl-Keles-Orhaneli çevresinin genel jeokimya raporu. Maden Tetkik ve Arama Genel Müdürlüğü Rapor No: 8179, Ankara (unpublished).
- Romberg, H. 1938. Bursa Vilayetinde Sebihtepe'de, Karaislak, Kuzbudak ve Keles'de Tetkik Olunan Yataklar Hakkında Rapor. Maden Tetkik ve Arama Genel Müdürlüğü Rapor No: 722, Ankara (unpublished).
- Sato, K. 1980. Tungsten Skarn Deposit of the Fujigatani Mine, Southwest Japan. Economic Geology 75, 1066-1082.
- Song, G., Qin, K., Li, G., Evans, N.J., Chen, L. 2014. Scheelite elemental and isotopic signatures: Implication for the genesis of skarn-type W-Mo deposits in the Chizhou Area, Anhui Province, Eastern China. American Mineralogist 99, 303-317.
- Sun, S.S., McDonough, W.F. 1989. Chemical and isotopic systematics of oceanic basalts: implications for mantle composition and processes. Saunders, A.D., Norry, M.J. (Eds.). Magmatism in ocean basins. Geological Society London. Special Publications 42, 313-345.
- Şengör, A.M.C., Yılmaz, Y. 1981. Tethyan Evolution of Turkey: A Plate Tectonic Approach. Tectonophysics 75, 181-241.
- Tekin, U.K., Göncüoğlu, M.C., Turhan, N. 2002. First evidence of Late Carnian radiolarians from the İzmir-Ankara suture complex, central Sakarya, Turkey: Implications of the opening age of the İzmir-Ankara branch of Neo-Tethys. Geobis 35, 127-135.
- Timon Sanchez, S.M, Moro Benito, M.C., Cembranos Perez, M.,L. 2009. Mineralogical and physiochemical evolution of the Los Santos scheelite skarn, Salamanca, NW Spain. Economic Geology 104, 961-995.
- Vander Auwera, J.V., Andre, L. 1991. Trace elements (REE) and isotopes (O, C, Sr) to characterize the metasomatic fluid sources: evidence from the skarn deposit (Fe, W, Cu) of Traversella (Ivrea, Italy). Contributions to Mineralogy and Petrology 106, 325-339.
- Whitney, P.R., Olmsted, J.F. 1998. Rare earth element metasomatism in hydrothermal system: The Willsboro-Lewis wollastonite ores, New York, USA. Geochimica et Cosmochimica Acta 62, 17, 2965-2977.
- Zaw, K., Singoyi, B. 2000. Formation of magnetite-scheelite skarn mineralization at Kara, Northwestern Tasmania: evidence from mineral chemistry and stable isotopes. Economic Geology 95, 1215-1230.